IET Generation, Transmission & Distribution

Special Issue: Advanced Data-Analytics for Power System Operation, Control and Enhanced Situational Awareness

IET Journals
The Institution of Engineering and Technology

Hybrid randomised learning-based probabilistic data-driven method for fault-induced delayed voltage recovery assessment of power systems

ISSN 1751-8687
Received on 2nd March 2020
Revised 15th April 2020
Accepted on 18th May 2020
E-First on 6th August 2020
doi: 10.1049/iet-gtd.2020.0402
www.ietdl.org

Chao Ren[1], Rui Zhang[2] ✉, Yuchen Zhang[2], Zhao Yang Dong[2]

[1]*Interdisciplinary Graduate School, Nanyang Technological University, Singapore, Singapore*
[2]*School of Electrical Engineering and Telecommunication, University of New South Wales, Sydney, Australia*
✉ *E-mail: rachelzhang.au@gmail.com*

Abstract: With a large number of inverter-interfaced renewable power generation, fault-induced delayed voltage recovery (FIDVR) events have become a serious threat to power system stability assessment. This study proposes a novel data-driven method based on probabilistic prediction, ensemble learning, and multi-objective optimisation programming (MOP) to rapidly predict the FIDVR severity index for real-time FIDVR assessment. Distinguished from the existing single machine learning (ML) algorithm data-driven method, the proposed method combines different randomised learning algorithms to acquire a more diversified ML outcome. The probabilistic prediction models the uncertainties existing in the prediction process, which quantifies the prediction confidence over a progressive observation window. Besides, the FIDVR can be evaluated through the time-adaptive framework to achieve the best FIDVR speed and accuracy with the MOP framework. The simulation results on the New England 10-machine 39-bus system display its preponderance over the single ML, and also demonstrate its better speed and accuracy performance in FIDVR assessment.

Nomenclature

Parameters

N_b	total quantity of system buses
T	considered voltage transient time frame
T_c	fault cleared time
$V_{i,0}$	pre-fault voltage magnitude of bus i
$V_{i,t}$	voltage magnitude of bus i at the time t
μ	threshold to incredible voltage deviation
$g(\cdot)$	efficient activation function
$\boldsymbol{W}$	ELM input weight vector mapping all input nodes with its hidden node
$\boldsymbol{\beta}$	output weight vector mapping the hidden layer node with the output nodes
b	biases
$\boldsymbol{H}^{\dagger}$	*Moore–Penrose* generalised inverse of the hidden layer output matrix
$\boldsymbol{d}$	vector concatenating the hidden layer outputs and the inputs
$\boldsymbol{t}$	output vectors of RVFL
E	quadratic error of RVFL
N	quantity of training samples
F	quantity of input features
Z	quantity of hybrid ensemble model predictors
D	original training samples
D^*	bootstrapped pairs samples
h_E, h_R	hidden nodes of ELM and RVFL
$\hat{y}_m(\boldsymbol{x}_i)$	prediction value of bootstrapped ELM
$\hat{y}_n(\boldsymbol{x}_i)$	prediction value of bootstrapped RVFL
y_{true}	true TVSI of training samples
e_{label}	training error
$\hat{e}_{e_{\text{label}}}$	predicted error
$\hat{y}(\boldsymbol{t}_i)$	predicted TVSI value
$\sigma^2(\boldsymbol{t}_i)$	prediction uncertainty modelling
$\hat{e}_{\text{model}}$	inherent model uncertainty of the TVSI predictor
$\hat{e}_{e_{\text{label}}}$	predicted error
$\hat{e}_{e_{\text{label}},\text{model}}$	inherent model uncertainty of the error predictor
$\hat{y}_{e_{\text{label}},m}(\boldsymbol{t}_i)$	prediction value of the bootstrapped ELM instances
$\hat{y}_{e_{\text{label}},n}(\boldsymbol{t}_i)$	prediction value of the bootstrapped RVFL instances
p_1, p_2	objectives in terms of error and speed
$\boldsymbol{M}$, $\boldsymbol{N}$	participation factors and are the number of ELM predictors and RVFL predictors
$\boldsymbol{U}$	stopping criterion thresholds
$T_{\max}$	maximum allowable prediction time

1 Introduction

1.1 Background

Fault-induced delayed voltage recovery (FIDVR) refers to that, being subjected to large disturbances such as short-circuit faults, the power system voltage fails to recover to the secure level (e.g. 90% of pre-disturbance voltage) within an acceptable timeframe [1]. The FIDVR situation can further aggravate system conditions and lead to cascading failure and even fast voltage collapse. It is a critical concern with a large number of inverter-interfaced renewable power generation [2], e.g. the wind power and photovoltaic, has been integrated, which needs the more stringent low-voltage-ride-through capability. Besides, the induction motors share a considerable portion of the loads, e.g. air conditioners. Following a fast fault-induced voltage dropping, the fast-recovering behaviour can prominently damage the voltage recovery performance [3, 4], such as drawing excessive reactive power from the grid. Due to the FIDVR threat on the high-level wind power systems, South Australia occurs a wide range blackout event, which results in considerable power generation loss [5].

Voltage stability and FIDVR are both concerned with the post-disturbance voltage behaviour, but they focus on different aspects. Following a disturbance, voltage stability refers to the ability of bus voltages to successfully recover to its pre-disturbance level or not, either stable or unstable. In comparison, FIDVR only considers the stable cases, and focuses on the time taken for the bus voltages to recover, which usually requires numerical metrics to evaluate its severity.

With the recent development of time-synchronised measurement techniques, real-time FIDVR assessment has been

identified as a sound solution for mitigating the FIDVR threat [6–9]. Following a large voltage disturbance, the FIDVR assessment should be accurate enough to avoid misoperation of control actions. Moreover, in the post-fault voltage propagation, the earlier the FIDVR event is detected, the higher chance the deviated voltage can be recovered timely. Therefore, the FIDVR assessment speed should also be valued seriously. The purpose of this paper is to balance and increase the accuracy and speed of real-time FIDVR assessment.

1.2 Literature review

The traditional evaluation methods for FIDVR are to simulate offline time-domain (T-D) on a pre-defined contingency set and solve a set of high-dimensional algebraic equations iteratively. It is difficult to meet the needs of real-time evaluation due to its high computational complexity, and it can only trigger emergency control actions in an event-based manner, making it less robust and inaccurate.

In recent years, a wide variety of machine learning-based (ML-based) data-driven methods, such as *Shapelet-based* classification [10], *Lyapunov exponent* method [11], imbalanced ML [12], multi-state classification [13] and wordbook-based light-duty time series learning machine [14], have been proposed for data-driven assessment. However, these conventional data-driven methods are based on a fixed long observation window [15] after the fault, which usually suffers from slow assessment speed. More recently, the time-adaptive framework has become popular in real-time assessment and has been applied in a wide range of areas such as transient stability assessment [16, 17], short-term voltage stability assessment [15], FIDVR assessment [18], and microgrid islanding detection [19]. Based on this framework, the evaluation progressively proceeds over the observation windows, and the final decision can be made at an appropriate earlier time based on the evaluated model credibility.

In our previous work [18], a probabilistic prediction framework is proposed for a time-adaptive FIDVR assessment. Compared to the deterministic mechanism in [15–17, 19], probabilistic prediction can not only provide the deterministic assessment result but also quantify the error in the assessment. Such FIDVR assessment on a probabilistic basis has been both theoretically and practically verified as a more accurate method to evaluate the model credibility in a time-adaptive decision process; thus, an early determination advantage of time-adaptive assessment can be more reliably achieved. However, some disadvantages of the existing method in [18] can be observed:

(i) The method in [18] can only make accurate binary decisions on FIDVR acceptability (i.e. whether a FIDVR event is acceptable or unacceptable) and lacks reliable numerical evaluation capability on FIDVR event.
(ii) The parameters involved in the ML model and probabilistic time-adaptive prediction are empirically determined without any optimisation on them, which could lead to sub-optimal performance of the method.
(iii) Only a single ML algorithm, random vector functional link neural network (RVFL), was adopted in [18] to achieve a probabilistic model. Its learning diversity for prediction error evaluation could be further reinforced by integrating multiple learning algorithms.

1.3 Contributions in this paper

Considering the above inadequacies, a new hybrid ensemble method for probabilistic learning is proposed. It can achieve probabilistic and time-adaptive time-series prediction for real-time FIDVR assessment, which can significantly improve both the assessment speed and accuracy. Distinguished from the existing single ML-based data-driven method, the proposed hybrid model combines different randomised ML algorithms, such as extreme learning machine (ELM) and RVFL, to acquire the multifarious ML outcomes for improved FIDVR assessment performance. Besides, the FIDVR is evaluated in an optimised way in order to acquire the optimally balanced FIDVR assessment accuracy and speed through a multi-objective optimisation programming (MOP). The main contribution and value of this paper are summarised as follows:

(i) The FIDVR severity is quantified by continuous transient voltage severity index (TVSI), and the real-time FIDVR assessment can be converted to a time series prediction problem. This allows the proposed method to provide a numerical evaluation on FIDVR events as its output. Compared to the binary decision-making in [18], the system operators can gain more accurate FIDVR assessment based on such numerical value.
(ii) A probabilistic time-adaptive method is designed based on the hybrid ensemble learning model to quantify the uncertainties in the prediction process. Under the time-adaptive framework, the FIDVR severity can be progressively predicted on a probabilistic basis via a hybrid ensemble learning model.
(iii) The hybrid ensemble learning model combines different randomised ML algorithms to improve diversity. The aggregated output can show its better performance than the single ML models.
(iv) The parameters involved in the hybrid ensemble model and probabilistic time-adaptive prediction process are optimised by solving a MOP to optimally balance the FIDVR assessment accuracy and speed. The performance of the proposed method can be assessed to satisfy different practical requirements by providing the optimal solution sets to the system operators.

The proposed method is tested on the New England 10-machine 39-bus system and shown significant improvement in FIDVR assessment speed and accuracy compared with the existing methods.

2 Problem descriptions

The proposed method belongs to a time-series prediction process that can predict the TVSI value. The FIDVR events should be assessed in a probabilistic time-adaptive prediction framework to improve the speed without sacrificing overall assessment accuracy. This section firstly introduces the TVSI as quantification of FIDVR severity, and then describes the time-adaptive prediction framework for FIDVR assessment; in the end, the shortcomings in existing methods are shown.

2.1 Transient voltage severity index

The severity of dynamic voltage deviation can be varying depending on the severity of disturbance, which needs appropriate metrics to evaluate such severity. A set of industrial criteria based on the voltage deviation magnitude and the associated duration time have been designed [20], i.e. if the duration time for the bus voltage to remain below 90% of its steady-state level exceeds a pre-defined threshold, the FIDVR event is identified as unacceptable and will trigger voltage control actions. Such rule-based industrial criteria show great differences among the operating regions, countries, the utilities, and lack quantitative evaluation on voltage recovery behaviour. Thus, there is a pressing need for a continuous index to quantify the FIDVR phenomenon. In practice, the magnitude of the voltage deviation and the associated duration time would serve as the two indicators of voltage deviation severity [15].

In this paper, TVSI proposed in [15] is utilised, which is a straightforward and numerical index

$$\mathrm{TVSI} = \frac{\sum_{i=1}^{N_b}\sum_{t=T_\mathrm{c}}^{T}\mathrm{TVDI}_{i,t}}{N_b \times (T - T_\mathrm{c})} \tag{1}$$

where N_b represents the total quantity of system buses, T represents the considered voltage transient time frame, T_c represents the fault cleared time, and TVDI represents the transient voltage deviation index, defined as follows:

$$\mathrm{TVDI}_{i,t} = \begin{cases} \dfrac{|V_{i,t} - V_{i,0}|}{V_{i,0}}, & \text{if } \dfrac{|V_{i,t} - V_{i,0}|}{V_{i,0}} \geq \mu \\ 0, & \text{otherwise} \end{cases} \quad \forall t \in [T_c, T] \quad (2)$$

where $V_{i,0}$ represents the pre-fault voltage magnitude of bus i, $V_{i,t}$ represents the voltage magnitude of bus i at time t, and μ represents the threshold to define incredible voltage deviation level, which is set at 10% according to the practical criteria [20].

TVSI aims to integrate the buses with unacceptable voltage violations in the transient period. TVSI takes into account both the voltage violation magnitude and the associated duration time in the whole system level. A smaller TVSI value indicates lower FIDVR severity, meaning a better voltage recovery performance [15]. Note that the load level indicates the operating range of the systems, and TVSI is used to quantify the severity of the post-fault voltage deviation.

2.2 Time-adaptive assessment framework

With the employment of synchronised measurement techniques and wide-area measurement systems, the voltage trajectory can be measured in real time; thus FIDVR can be predicted by the voltage trajectories. Under such sensing infrastructure, the FIDVR assessment speed represents the elapsed time from the fault clearance time to the assessment prediction time.

The aim of the time-adaptive prediction framework [16] is to improve the classification/regression speed of a time-series without impairing the overall accuracy. In order to improve the prediction speed, a probabilistic time-adaptive FIDVR assessment method is proposed, which can progressively predict the TVSI value by using the real-time voltage data measured from each time point.

To acquire a better performance, ML algorithms would be applied to predict the TVSI based on the real-time voltage trajectories. By comparing the predicted TVSI with the default threshold, the system can make the corresponding decision. If the predicted TVSI is higher than the default threshold, the FIDVR event is regarded as incredible. But if the stopping criterion threshold is too small, the assessment speed would be too slow to trigger emergency control action on time.

Applying for the FIDVR assessment problem, the proposed method of this framework is illustrated in Fig. 1. There are a series of intelligent models, and each of them operates at a different time point T_i. For each time point T_i, check the prediction uncertainty to decide whether the result is confidence: if the output is identified as a credible event, the result will be directly obtained at the current time point; otherwise, such assessment will continue at the next time point T_{i+1}. The whole process proceeds until a confident FIDVR assessment result can be obtained or the maximum allowable prediction time is reached.

Compared with traditional fixed-time methods [10–15], the time-adaptive assessment framework can take the temporal voltage value dependency into consideration and reliably deliver the final decision as early as possible. According to [16–19], the overall prediction assessment speed is significantly improved by such a time-adaptive mechanism.

2.3 Inadequacies of existing methods

Considering the practical need for real-time FIDVR assessment, the assessment accuracy and speed are the significant criteria to evaluate the FIDVR assessment performance. Generally, the longer the response time, the more information can be measured, then the FIDVR assessment result tends to be more confident. The current fixed-time FIDVR assessment methods [9, 10, 15] only pursue the high accuracy, but neglect the speed. Under these circumstances, the assessment results might be obtained too late to activate emergency control in time against the risk of blackouts.

Another shortcoming is that the existing time-adaptive framework utilises a large quantity of user-defined parameters that must be manually tuned based on practical experience [13, 15, 20–22]. These human-experienced works are time-consuming and can easily lead to a sub-optimal solution. Thus, there is a press needing to design an autonomous model to optimise the time-adaptive assessment framework. It can be clearly observed that there is a trade-off in terms of the assessment accuracy and speed, so how to balance this trade-off should also be paid more attention.

3 Proposed method

Randomised ML algorithms are excellent candidates for ensemble learning for their naturally diverse. Compared to the deterministic mechanism in [15–17, 19], a new hybrid ensemble probabilistic learning is designed for achieving probabilistic and time-adaptive time-series prediction for real-time FIDVR assessment via a MOP to balance FIDVR assessment accuracy and speed through, which can significantly improve both the assessment speed and accuracy. This section firstly introduces the randomised learning algorithms, then designs an intelligent model and the uncertainty from predictor and noise. Finally, in order to balance the speed and accuracy, the model is optimised to achieve the optimal FIDVR assessment.

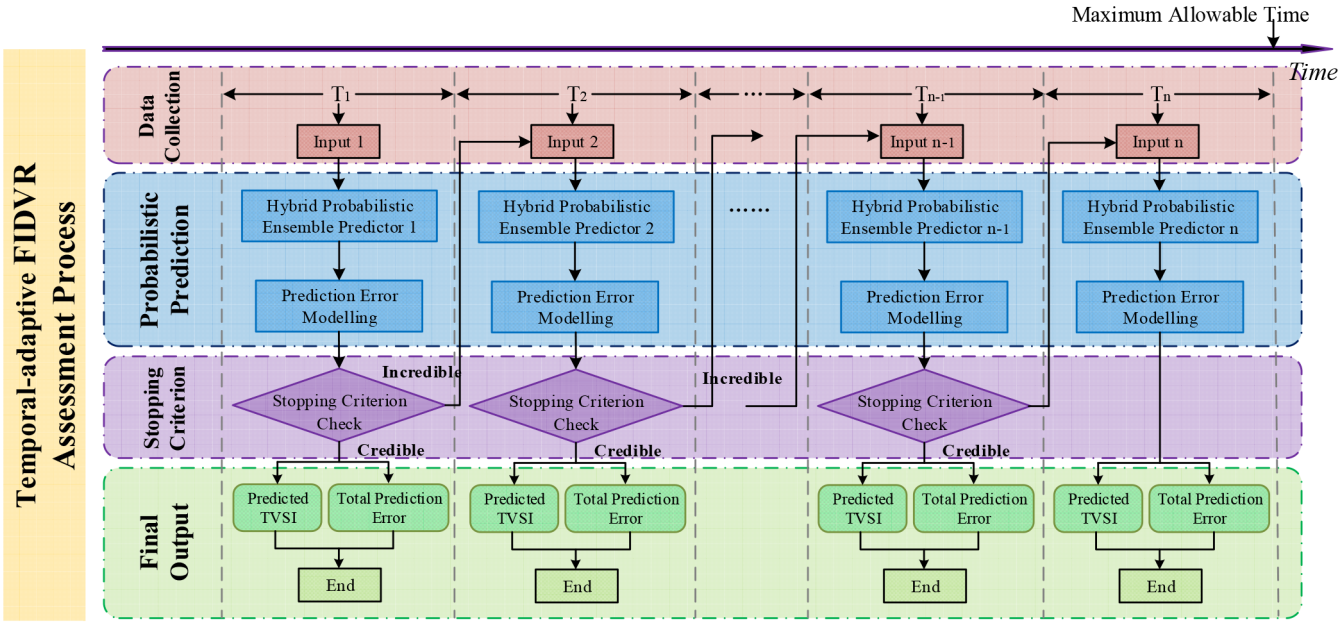

Fig. 1 *Time-adaptive prediction framework for FIDVR assessment*

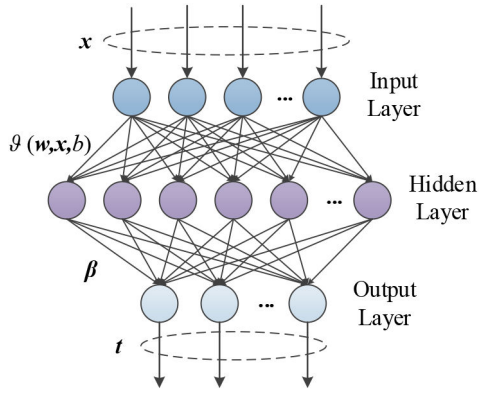

Fig. 2 *Basic structure of ELM*

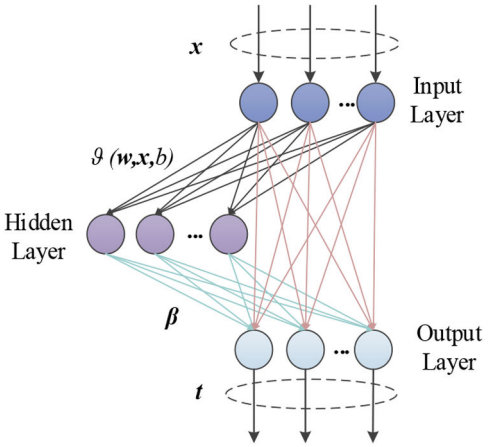

Fig. 3 *Basic structure of RVFL*

3.1 Randomised ML algorithms

Randomised ML algorithms refer to a single hidden layer feed-forward network (SLFN) with randomised input weights and biases [23], which are naturally diverse and show fast learning capability on classification/prediction tasks. Among them, ELM and RVFL are two kinds of popular randomised ML algorithms.

3.1.1 Extreme learning machine: ELM belongs to a generalised SLFN, and it has become very popular in the academic and practical industry [24]. The structure of ELM consists of an input layer, a hidden layer, and an output layer, as shown Fig. 2.

For a basic ELM, the outputs can be formulated as follows:

$$f_{\tilde{N}}(x_j) = \sum_{i=1}^{\tilde{N}} \boldsymbol{\beta}_i \cdot g(\boldsymbol{w}_i \cdot \boldsymbol{x}_j + b_i) = t_j, \quad j = 1, 2, \ldots, N \tag{3}$$

where $g(\cdot)$ is the efficient activation function, $\boldsymbol{W}_i$ represents the input weight vector mapping all input nodes with its hidden node, $\boldsymbol{\beta}_i$ represents the output weight vector mapping the ith hidden layer node with the output nodes and b_i represents the biases at the ith hidden layer node.

At the training process, the weights and biases of the ELM are randomly chosen; such a structure can avoid iterative training procedure. After that, analytically obtain the output weights β by direct matrix calculations. If the quantity of hidden layer nodes is much less than the number of training samples, it will become a linear system for fixed $\boldsymbol{w}_i$ and b_i, and output weight $\boldsymbol{\beta}^*$ is calculated via the minimal norm least square as follows:

$$\boldsymbol{\beta}^* = \boldsymbol{H}^{\dagger}\boldsymbol{T} \tag{4}$$

where $\boldsymbol{H}^{\dagger}$ is the *Moore–Penrose* generalised inverse of the hidden layer output matrix.

Compared to the traditional ML algorithms, e.g. backpropagation, ELM can randomly select its parameters, which can significantly decrease the training computation burden and improve much training speed. Other advantages of ELM are its less need for parameter tuning and excellent generalisation ability, such as stopping criteria design and learning rate settings that are commonly encountered in the traditional neural networks.

3.1.2 Random vector functional link neural network: RVFL shown in Fig. 3 also belongs to the randomised neural network. The specific characteristic of RVFL is its direct input–output connection. Based on such a structure, the output can be formulated as follows:

$$\boldsymbol{t}_i = \boldsymbol{d}_i^{\mathrm{T}}\boldsymbol{\beta}, \quad i = 1, 2, \ldots, R \tag{5}$$

where R represents the number of samples, $\boldsymbol{d}_i$ represents a vector concatenating the hidden layer outputs and the inputs, $\boldsymbol{\beta}$ represents the output weight vector, and $\boldsymbol{t}_i$ represents the output vector. The weights mapping the input to the hidden layer nodes are randomly chosen within the appropriate domain via the obtained scale factor in the parameter adjustment phase, and such weights are generated uniformly. The RVFL learning procedure can be formulated into the minimisation of the quadratic error E as follows:

$$E = \frac{1}{2R}\sum_{i=1}^{R}(\boldsymbol{t}_i - \boldsymbol{\beta}^{\mathrm{T}}\boldsymbol{d}_i)^2 \tag{6}$$

The input weights and biases are randomly chosen in a suitable domain, so RVFL has a fast learning capability as ELM. Moreover, RVFL has a direct input–output connecting structure, which is the main difference between ELM and RVFL. With such a structure, RVFL can map both non-linear and linear relationships between inputs and outputs, which can help to regularise the error caused by the randomly chosen input weights and biases [25].

3.2 Bootstrap methods

Bootstrap belongs to the general statistics inference approach, which can be applied for regression analysis. Bootstrap generates sampling distributions by using uniform sampling, which is used for replacing the original data. It is widely utilised as a robust alternative to the statistical inference based on the parametric assumptions because it is difficult to compute the standard errors in some sophistication conditions.

As to the pairs bootstrap method, when training a randomised learning neural network on particular bootstrap samples, the model parameters are estimated so as to minimise the errors on the training data. Based on the bootstrap duplicates, the model can be trained and obtain corresponding outputs for regression analysis.

3.3 Hybrid ensemble model via randomised learning

Ensemble learning algorithms can solve the same regression/classification problem by combining different ML units. With such a paradigm, the whole model can be more diverse, and its ensembling output would be more robust and more accurate, which has been demonstrated in [26–28].

Since the randomised networks are stochastic in nature, uncertainties are inevitably generated in their learning outcome. In the proposed method, such an uncertainty problem has been overcome by adopting hybrid ensemble learning models, to obtain a more diversified machine learning outcome for improved FIDVR performance. This paper designs a new hybrid ensemble model for real-time FIDVR assessment. The hybrid model ensembles RVFL and ELM as the single ML units so as to construct the hybrid ensemble model for achieving probabilistic prediction, which can both improve the accuracy and supply the potential prediction and prediction error to make more reliable mechanism before failure [26, 27].

Since the training speed of RVFL and ELM can be effectively improved, hence, the computational burden of ensemble learning

Input: Given a database of $N\times F$ size to train Z predictors, including m ELMs and n RVFLs ($m+n=Z$), where N is the quantity of training samples and F is the quantity of input features.

Output: The hybrid ensemble learning model.

Begin

Obtain the original training samples $D_t=\{(\mathbf{x}_1, \mathbf{t}_1),\ldots,(\mathbf{x}_N, \mathbf{t}_N)\}$.

Randomly select $f\in[1, F]$ in the features.

For $i=1$ to E:

1) Generate N bootstrapped pairs $D_t^*=\{(\mathbf{x}_1^*, \mathbf{t}_1^*),\ldots,(\mathbf{x}_N^*, \mathbf{y}_N^*)\}$ via uniform sampling with replacement from the original training samples $D_t=\{(\mathbf{x}_1, \mathbf{t}_1),\ldots,(\mathbf{x}_N, \mathbf{t}_N)\}$.
2) Randomly allocate ELM hidden nodes h_E within an optimal hidden nodes range $[h_{MIN}, h_{MAX}]$ (Subject to a tuning process).
3) Randomly allocate RVFL hidden nodes h_R within an optimal hidden layer nodes range $[h_{MIN}, h_{MAX}]$ (Subject to a pre-tuning process).
4) Train the ELM or the RVFL via the N bootstrapped pairs D_t^* samples, features, the number of hidden nodes, and activation function.

End For

Obtain bootstrap replicates and hybrid ensemble learning model.

End

Fig. 4 *Algorithm 1: hybrid ensemble learning model*

can be significantly alleviated, which reduces the overall training time of the FIDVR assessment models. Moreover, in the ensemble process, different randomised learning algorithms can involve randomness, which can improve robustness and the generalisation ability of the hybrid ensemble model.

In the proposed hybrid ensemble learning model, the training data for each single learning unit is generated via a pair bootstrap method. The hybrid ensemble model training process can be summarised in Algorithm 1 (see Fig. 4).

3.4 Probabilistic prediction framework

The prediction construction for forecasting is designed via the pair bootstrap method. The probabilistic predictor should be carefully designed because it would determine the overall prediction accuracy and response time. The uncertainties of a hybrid ensemble model-based probabilistic prediction are mainly in virtue of the deviation of the hybrid ensemble model for regression analysis and the noise of training samples.

3.4.1 Predictor uncertainty in a hybrid ensemble model: Deviations in hybrid ensemble model structure and parameters would lead to the uncertainty of neural network forecasting, which are mainly due to the randomly generated input weights or biases, local minima in the training process, and so on. Therefore, the output uncertainty of neural networks should be well computed in order to obtain accurate estimation.

The bootstrap-based method assumes that the proposed hybrid ensemble model will achieve true regression analysis of the measured targets with less biased approximation. Given the original training samples $D_t=\{(\boldsymbol{x}_1, \boldsymbol{t}_1), \ldots, (\boldsymbol{x}_N, \boldsymbol{t}_N)\}$. The hybrid ensemble model which uses the TVSI as the targets follows the single learning unit training, the average output of the ensemble of m ELMs and n RVFLs can be computed as the standard estimation of the true regression, and the formula is as follows:

$$\hat{y}(\boldsymbol{x}_i)=\frac{1}{m+n}\left[\sum_{m=1}^{m}\hat{y}_m(\boldsymbol{x}_i)+\sum_{n=1}^{n}\hat{y}_n(\boldsymbol{x}_i)\right] \tag{7}$$

where m ELMs and n RVFLs training data sets are replicated by following the pairs bootstrap procedure with the original training samples, $\hat{y}_m(\boldsymbol{x}_i)$ and $\hat{y}_n(\boldsymbol{x}_i)$ represent the prediction value of the input instances generated by bootstrapped ELMs and bootstrapped RVFLs, respectively. The corresponding training errors are extracted as follows:

$$e_{\text{label}}=\sigma_{\hat{y}}^2(\boldsymbol{x}_i)=\left(y_{\text{true}}(\boldsymbol{x}_i)-\hat{y}(\boldsymbol{x}_i)\right)^2 \tag{8}$$

where y_{true} and e_{label} are the true TVSI of training samples and the training error, respectively.

3.4.2 Noise uncertainty in the database set: If the database sets have random properties, it is very difficult to model them in a deterministic way. Particularly when dealing with non-stationary time series, data noises have a great influence on prediction results.

The predicted TVSI is the mean output from a single learning unit based on a hybrid ensemble model in the TVSI predictor as

$$\hat{y}(\boldsymbol{t}_i)=\frac{1}{m+n}\left[\sum_{m=1}^{m}\hat{y}_m(\boldsymbol{t}_i)+\sum_{n=1}^{n}\hat{y}_n(\boldsymbol{t}_i)\right] \tag{9}$$

where $\hat{y}(\boldsymbol{t}_i)$ is the predicted TVSI value.

The prediction uncertainty is modelled via (1) the expected error between the prediction error and the real target value, and (2) the inherent model uncertainty of ML model [18]. Thus, the prediction uncertainty modelling $\sigma^2(\boldsymbol{t}_i)$ totally includes two parts with three components: the output variance $\hat{e}_{\text{model}}$ to evaluate the inherent model uncertainty of the TVSI predictor, the average output $\hat{e}_{e_{\text{label}}}$ to evaluate predicted error and the output variance $\hat{e}_{e_{\text{label}},\text{model}}$ to evaluate the inherent model uncertainty of the error predictor. Those three components can be mathematically calculated as follows:

$$\begin{aligned}\sigma^2(\boldsymbol{t}_i)&=\hat{e}_{\text{model}}+\hat{e}_{e_{\text{label}}}+\hat{e}_{e_{\text{label}},\text{model}}\\&=\sigma_{\hat{y}}^2(\boldsymbol{t}_i)+\hat{e}_{e_{\text{label}}}+\sigma_{\hat{y}_{e_{\text{label}}}}^2(\boldsymbol{t}_i)\end{aligned} \tag{10}$$

where

$$\begin{aligned}\hat{e}_{\text{model}}=\sigma_{\hat{y}}^2(\boldsymbol{t}_i)=\frac{1}{m+n-1}\Bigg[&\sum_{m=1}^{m}\left(\hat{y}_m(\boldsymbol{t}_i)-\hat{y}(\boldsymbol{t}_i)\right)^2\\&+\sum_{n=1}^{n}\left(\hat{y}_n(\boldsymbol{t}_i)-\hat{y}(\boldsymbol{t}_i)\right)^2\Bigg]\end{aligned} \tag{11}$$

$$\hat{e}_{e_{\text{label}}}=\frac{1}{m+n}\left[\sum_{m=1}^{m}\hat{y}_{e_{\text{label}},m}(\boldsymbol{t}_i)+\sum_{n=1}^{n}\hat{y}_{e_{\text{label}},n}(\boldsymbol{t}_i)\right] \tag{12}$$

$$\begin{aligned}\hat{e}_{e_{\text{label}},\text{model}}=\sigma_{\hat{y}_{e_{\text{label}}}}^2(\boldsymbol{t}_i)=\frac{1}{m+n-1}\Bigg[&\sum_{m=1}^{m}\left(\hat{y}_{e_{\text{label}},m}(\boldsymbol{t}_i)-\hat{e}_{e_{\text{label}}}\right)^2\\&+\sum_{n=1}^{n}\left(\hat{y}_{e_{\text{label}},n}(\boldsymbol{t}_i)-\hat{e}_{e_{\text{label}}}\right)^2\Bigg]\end{aligned} \tag{13}$$

where $\hat{y}_{e_{\text{label}},m}(\boldsymbol{t}_i)$ and $\hat{y}_{e_{\text{label}},n}(\boldsymbol{t}_i)$ represent the prediction value of the output instances, which are generated by bootstrapped ELMs and bootstrapped RVFLs with the training errors e_{label}, respectively. As random noises are existed in both the training process, the predicted error $\hat{e}_{e_{\text{label}}}$ has a corresponding impact on the measurement noise; hence, influences the prediction accuracy. The probabilistic prediction construction is highly reliable, verified by the low average coverage error index.

3.5 Optimal accuracy-speed balancing

As shown previously, there should be a trade-off between FIDVR assessment accuracy and speed. Besides, the overall assessment performance under a time-adaptive prediction is sensitive to two sets of parameters, including the stopping criterion thresholds and the participation factors of ELM and RVFL. The trade-off relationship can be modelled as a MOP, based on which the stopping criterion thresholds and the participation factors are optimised to achieve the optimal FIDVR assessment accuracy and speed.

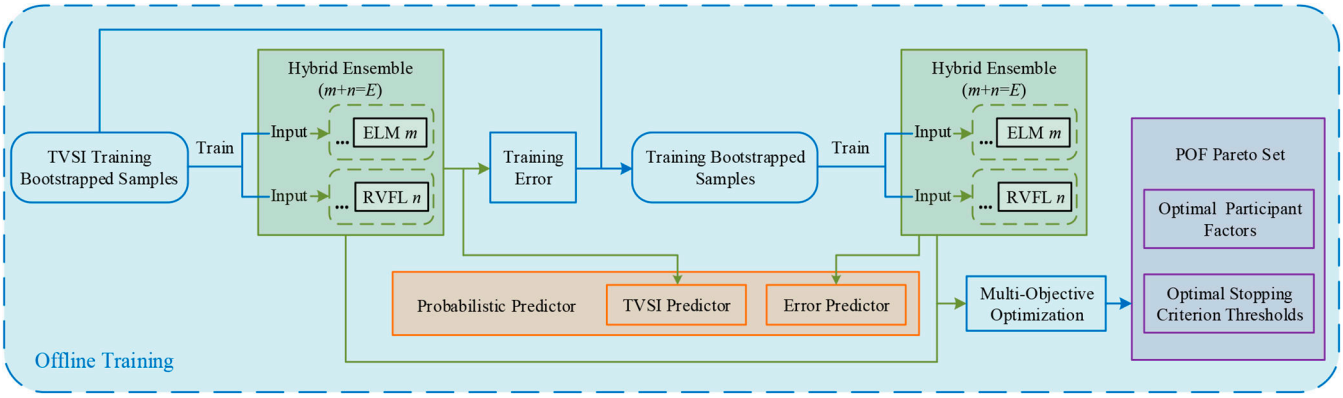

Fig. 5 *Offline training procedures of the proposed method*

3.5.1 Multi-objective optimisation programming: The MOP for balancing the assessment speed and error is defined as follows:

$$\text{Objectives}: \underset{\boldsymbol{x}}{\text{Maximise}} \quad \boldsymbol{p}(\boldsymbol{x}) \tag{14}$$

where

$$\boldsymbol{x} = [\boldsymbol{U}, \boldsymbol{M}, \boldsymbol{N}]$$
$$\begin{cases} \boldsymbol{U} = (u^1, u^2, u^3, \ldots, u^{T_{\max}}) \\ \boldsymbol{M} = (m^1, m^2, m^3, \ldots, m^{T_{\max}}) \\ \boldsymbol{N} = (n^1, n^2, n^3, \ldots, n^{T_{\max}}) \end{cases} \tag{15}$$

$$\boldsymbol{p}(\boldsymbol{x}) = [p_1(\boldsymbol{x}), p_2(\boldsymbol{x})] = [Error, Speed] \tag{16}$$

where the error and speed are the two objectives related to the stopping criterion thresholds and the participation factors of ELM and RVFL through p_1 and p_2, respectively. $\boldsymbol{M}$ and $\boldsymbol{N}$ belong to participation factors and are the number of ELM predictors and RVFL predictors for each time point, respectively; $\boldsymbol{U}$ belongs to the stopping criterion thresholds for each time point and represents the practical total prediction uncertainty thresholds to distinguish credible and incredible FIDVR case. Under the time-adaptive FIDVR assessment framework, the quantity of decision parameters relies on the maximum allowable prediction time $T_{\max}$. Overall, combining the stopping criterion thresholds with participant parameters, the constraints are as follows:

$$\text{Constraints}: m^k + n^k = Z \tag{17}$$

$$u^k \geq 0 \tag{18}$$

$$1 \leq k \leq T_{\max} \tag{19}$$

By solving such MOP, system operators can select the best solutions according to the practical requirements.

3.5.2 FIDVR assessment performance metrics: In order to optimise the FIDVR assessment, appropriate metrics should be utilised to quantify the FIDVR assessment performance. Since real-time FIDVR assessment belongs to a time series prediction question, the mean absolute percentage error (MAPE) is adopted in this paper to evaluate the prediction error at each time point. The MAPE formulation is as follows:

$$\text{MAPE}(T) = \frac{\sum_{i=1}^{d} |y_{\text{true}} - \hat{y}(T)|}{|y_{\text{true}}| \cdot d} \tag{20}$$

where T is a time point, y_{true} and $\hat{y}$ are the true and predicted TVSI value, respectively, and d is the accumulated number of credible testing instances up to the time point T.

Since we aim to accurately assess all instances and effectively improve the assessment speed, the average prediction speed (APS) and average prediction error (APE) are defined as the performance indices for the proposed method:

$$\text{APS} = \frac{1}{T_{\text{total}}} \cdot \sum_{i=1}^{r} [T_i \times C(T_i)] \tag{21}$$

$$\text{APE} = \frac{1}{T_{\text{total}}} \cdot \sum_{i=1}^{r} [C(T_i) \times \text{MAPE}(T_i)] \tag{22}$$

where r and T_{total} are the total quantity of time points and samples; T_i represents the ith time point; T_{total} represents the total instances; $C(T_i)$ is the total quantity of credible samples at the current time point.

In FIDVR assessment with credible prediction, the APS measures the total FIDVR speed, and the APE measures the overall MAPE. By optimising the values of the stopping criterion thresholds and the predictors' participant factors, APS and APE can be optimally balanced.

3.5.3 Pareto optimisation: The trade-off relationship can be interpreted by the Pareto optimality theory. Given a set of optimised solutions, system operators can utilise one of the most suitable solutions considering the various practical situations. The set of all Pareto optimal solutions is named the Pareto set, and the set of all Pareto optimal target vectors forms the *Pareto optimal frontier* (POF). By using POF, an interpretable and remarkable pattern showing the trade-off between average FIDVR assessment error and average response time can be displayed. The final selection of the most suitable parameters set from the Pareto set can be decided via the practical industrial needs of system operators.

4 Implementation of the proposed method

The proposed method consists of two stages, including an offline training process and an online application process, which are illustrated in Figs. 5 and 6.

4.1 Offline training process

The proposed probabilistic predictor is composed of two hybrid ensemble models, including a TVSI predictor which is employed to deterministically predict the TVSI based on the incoming trajectory snapshot, and an error predictor which is applied to compute the error between the true and the predicted TVSI. The purpose of the proposed probabilistic predictor is to utilise the diversified and multiple ensemble outputs to statistically evaluate the prediction results. During the offline process, TVSI predictor and error predictor are sequentially trained as follows: a TVSI predictor is trained as a regression model using the original database $D_t = \{(\boldsymbol{x}_1, \boldsymbol{t}_1), \ldots, (\boldsymbol{x}_N, \boldsymbol{t}_N)\}$, then an error predictor is trained as a regression model using a modified database, which is to replace the TVSI values of each sample by the optimised training error e_{label} of TVSI predictor as the error predictor training target.

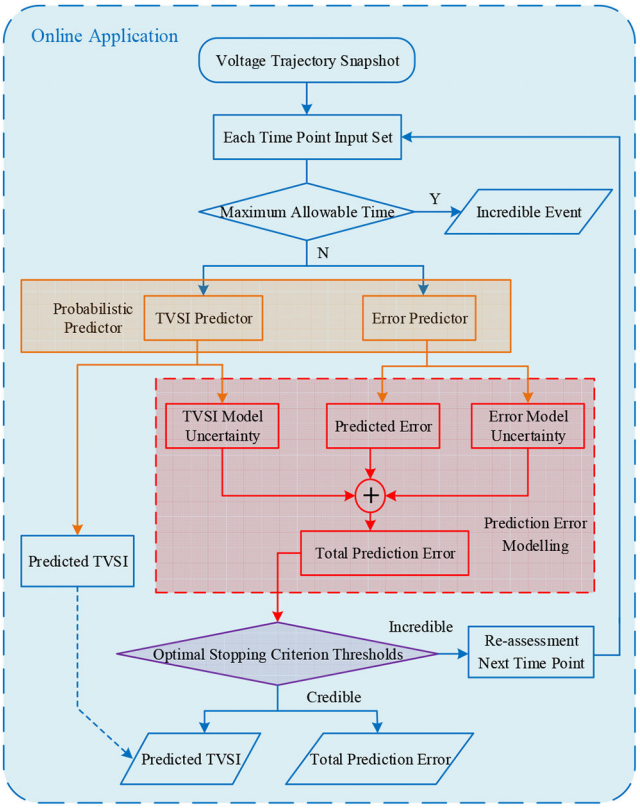

Fig. 6 *Online application procedures of the proposed method*

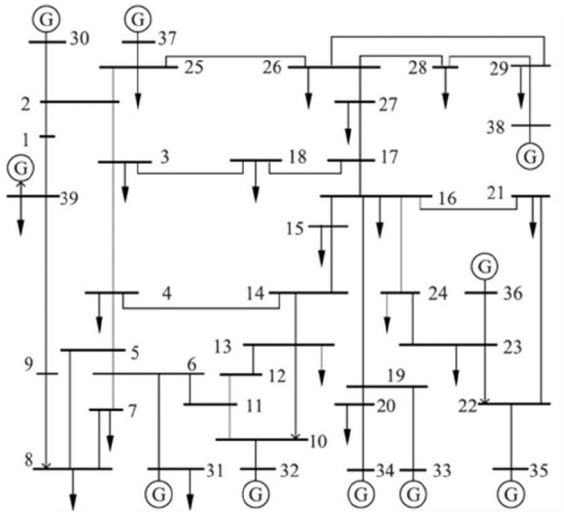

Fig. 7 *Single-line diagram of New England 10-machine 39-bus system*

For the proposed probabilistic predictor, the input and output specifications of the involved ELM and RVFL are as follows: The input in the TVSI predictor and error predictor is the same (i.e. the post-fault voltage trajectory snapshot). However, due to the different roles of the two hybrid ensemble models, their ELM/RVFL has different output specifications. The output in the TVSI predictor is the predicted TVSI value, while the output in the error predictor is the expected error between the true and the predicted TVSI.

Since such MOP is formulated based on the credible outputs from the hybrid ensemble learning model, TVSI predictor and error predictor both are designed to derive the POF. The whole stopping criterion thresholds and participation factors in the time-adaptive scheme should be optimised. Finally, the trained hybrid ensemble, the POF, and the Pareto set can form a reliable and effective probabilistic predictor, including TVSI predictor and error predictor for online application.

In performance optimisation, the TVSI bootstrapped training samples outputs and error bootstrapped training sample both construct new multiple and diversified output set by combining ELM and RVFL, based on which the MOP is solved to search for the optimal FIDVR performance. This paper applies NSGA-II [29] to copy with the MOP, and the corresponding POF can be calculated as the optimal result. Due to multiple Pareto points with equal optimality, a compromise solution can be chosen among them to represent the best FIDVR performance. In general, such a compromise solution is decided according to the practical need, e.g., maximum accuracy or minimum speed.

4.2 Online application process

At the online application stage, FIDVR is evaluated based on the trajectory snapshot measured at each time point. The FIDVR of incoming samples is assessed in a time-adaptive scheme via the optimal parameters trained in the offline process. Although the probabilistic predictor should enclose both the predicted TVSI and the prediction error, these two parts are different and need to be computed separately during the online application process.

TVSI predictor is responsible to predict its TVSI values $\hat{y}(\boldsymbol{t}_i)$ and TVSI model uncertainty $\hat{e}_{\text{model}}$, and the error predictor is responsible to estimate the predicted error $\hat{e}_{e_{\text{label}}}$ and error model uncertainty $\hat{e}_{e_{\text{label}},\text{model}}$. Here, the TVSI value is a numerical quantity to describe the trend of the voltage to propagate into the credible level, and TVSI model uncertainty, predicted error and error model uncertainty constitute the prediction uncertainty model $\sigma^2(\boldsymbol{t}_i)$ by adding them together.

The hybrid ensemble model at the online stage can achieve the best accuracy based on the optimal participant factors, and the optimised credible prediction uses the optimal stopping criterion thresholds to achieve the best FIDVR performance. At each time point, the confident event output would be obtained with TVSI prediction $\hat{y}(\boldsymbol{t}_i)$ and its corresponding to total prediction uncertainty $\sigma^2(\boldsymbol{t}_i)$. If the result is credible, and the final decision will be directly sent as the ultimate FIDVR assessment decision, if not, the samples with incredible outputs are delivered to the next decision cycle for re-assessment.

5 Case study and discussion

The proposed FIDVR assessment model has been tested on the New England 10-machine 39-bus system (see Fig. 7) to verify its effectiveness on large systems further. The numerical simulation is conducted on a high-performance computer with an Intel Core i7 CPU and 32-GB RAM. The T-D simulation and real-time testing environment are implemented in a Transient Security Assessment Tool (TSAT). The proposed methods are applied for the MATLAB.

5.1 Database generation

To acquire a comprehensive database for FIDVR severity assessment, the uncertainties of various factors are considered, including the fault characteristics, the load composition, and the pre-fault operating point. These factors are set according to the practical circumstances and their changes. In order to consider the influence of wind power generation on FIDVR, the generator on bus 37 is substituted by the same power rating wind farm [18].

- *Pre-fault operating points:* 4962 operating points are generated by randomly varying the wind power output between 0 and its power rating. Besides, the load demand is set between 0.8 and 1.2 of its base values. Optimal power flow is run to dispatch the synchronous generation.
- *Load modelling:* An industry-standard composite load model 'CLOD'[30] used in PSS/E is applied in this paper. 'CLOD' consists of 6 load types, including small motors, large motors, discharge lighting, transformer saturation, and voltage-dependent loads, all of which are typical load components in practical substations. For each generated operating point, the portion of motor loads is randomly sampled between 0 and 80%,

and the different load components share can be obtained via measurement-based load modelling methods [31].

- *Fault types and fault duration:* Three-phase faults are considered in the simulation with the random fault duration (0.1–0.3 s). Moreover, the fault location is either a bus or a transmission line that is randomly selected from the system topology. Considering the actual industry scenarios, the fault would be cleared either with the transmission line tripping or without loss of power grid component. In doing so, various fault-induced topology changes have been considered.

Finally, the FIDVR dataset of 4962 instances (i.e. 4962 sets of post-fault voltage trajectories with their calculated TVSI values) is obtained through T-D simulation. The step size of the T-D simulation can be set to be 0.05 s so as to simulate the actual phasor measurement unit (PMU) frequency. Moreover, four sets of voltage waveforms in the database are extracted and shown in Figs. 8*a–d* to illustrate the post-disturbance voltage recovery behaviour under different TVSI values.

5.2 Setup for the time-adaptive hybrid model

- *Maximum allowable prediction time T_{max}:* Among the time-adaptive process, the structure should define a maximum allowable prediction time to guarantee the whole intelligent system more reliable. Therefore, $T_{\max}$ is set as 20 [27]. With such a setting, the probabilistic predictors are performed 20 times.
- *Time points:* In this case study, each time point is set as 0.05 s, and we train the hybrid ELM and RVFL ensemble predictor for each time point. Longer time points can improve FIDVR assessment accuracy, but it would leave less time for emergency control. Since the maximum allowable response time is 20-time points (1.0 s), the proposed method consists of a total of 20 hybrid ELM and RVFL ensemble predictors.
- *Quantity of RVFLs and ELMs in the ensemble E:* The existing research have proved that with the increasing of the number of ML units, the prediction error will be gradually reduced and converges to a limit [27, 29, 31], but increases the offline training burden. Based on the literature results, E is set as 200.
- *Activation function and optimal hidden layer nodes range:* In this case study, the sigmoid function is set as an activation function for ELM and RVFL predictors, which can reach the maximum classification accuracy. Besides, the common hidden nodes range for ELM and RVFL is [150, 250], which is an optimal hidden layer nodes range.
- *Number of training samples and testing samples:* The quantity of samples trained for RVFLs and ELMs determines the overall performance of the robustness. Thus, the training samples and testing samples are chosen to be 3970 (80%) and 992 (20%) as the literature, respectively.

5.3 Probabilistic prediction results

To validate the enhanced FIDVR results of the proposed method, the single ELM ensemble models and the single RVFL ensemble models are also tested for comparison. Besides, the time-adaptive prediction mechanism is employed for all the testing ensemble models, in order to make a pure comparison.

In probabilistic prediction performance optimisation, the MOP can be solved via NSGA-II and the Pareto solutions of three different models are displayed in Fig. 9. The important information of the two extreme points based on three different ensemble model POF is listed in Tables 1 and 2.

In Fig. 9, it is obvious that there is the trade-off relationship between FIDVR speed and error, and most of the Pareto points of hybrid ensemble probabilistic prediction model outperforms the single ELM ensemble models and the single RVFL ensemble models in terms of response time and error, so the proposed hybrid model can provide the improvement in FIDVR assessment results. In practice, the decision-maker can select a compromise solution according to the practical need, e.g. the required error or speed. The smaller the APE, the less MAPE and the higher accuracy.

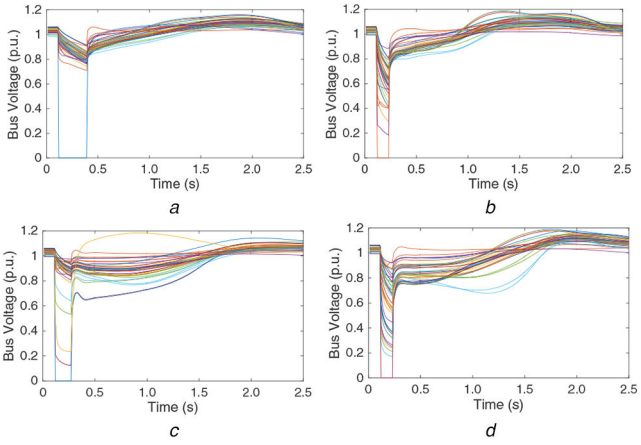

Fig. 8 *Examples of four FIDVR scenarios under different TVSI values*
(a) TVSI = 0.529, ***(b)*** TVSI = 1.509, ***(c)*** TVSI = 2.678, ***(d)*** TVSI = 3.267

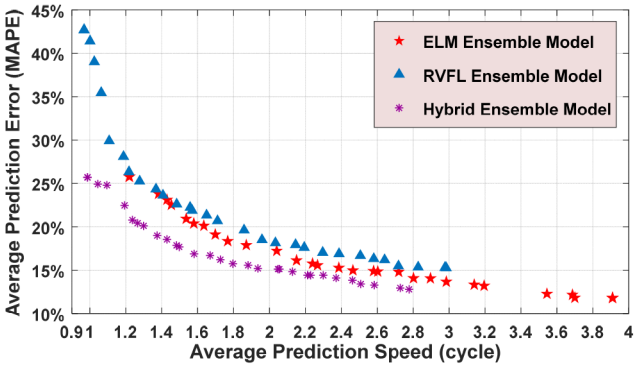

Fig. 9 *POF obtained in performance optimisation*

Table 1 Extreme Pareto points with the best APE

Ensemble model	No. of Pareto solutions	Worst case APS	Best case APE, %
single RVFL	29	2.984 cycles (0.1492 s)	15.26
single ELM	30	3.910 cycles (0.1955 s)	11.79
hybrid ELM and RVFL	28	2.777 cycles (0.1389 s)	12.80

Table 2 Extreme Pareto points with best APS

Ensemble model	No. of Pareto solutions	Best case APS	Worst case APE, %
single RVFL	29	0.968 cycles (0.0484 s)	42.70
single ELM	30	1.220 cycles (0.0610 s)	25.77
hybrid ELM and RVFL	28	0.987 cycles (0.0494 s)	25.70

Compared with the other two single ensemble models (ELM and RVFL), the proposed hybrid ensemble probabilistic predictor shows the best performance that response speed is slightly fastest and the average prediction error is smallest in both best APE case and best APS case.

In real-time FIDVR assessment, error and efficiency are both significant. High FIDVR assessment efficiency is especially significant when the system occurs a fast voltage collapse, and low error can serve as a basic requirement for FIDVR assessment. For the error and efficiency, the validation results shown in Fig. 9 demonstrate the importance of combining various ML algorithms instead of a single ML unit.

Table 3 Detail of the true TVSI value and predicted TVSI

FIDVR case ID	Predicted TVSI At T_1	Predicted TVSI At T_5	Predicted TVSI At T_{10}	Predicted TVSI At T_{19}	True TVSI
40	2.371	2.426	2.354	2.122	2.109
41	0.989	0.864	0.779	0.803	0.812
42	0.104	0.084	0.081	0.088	0.053
43	0.039	0.029	0.028	0.022	0.045
44	2.411	2.406	2.319	2.280	2.233
45	1.776	1.695	1.517	1.584	1.576
46	0.061	0.054	0.038	0.035	0.026

Table 4 Selected hybrid ensemble model Pareto point

Average prediction speed (time point)	Average prediction error (MAPE)
2.728 cycles (0.1364 s)	12.95%

Table 5 Online application testing results

Decision time cycles	Number of remained samples	Number of evaluated samples	Each decision cycles error, %
1 (0.05 s)	992	67	23.04
2 (0.10 s)	925	257	14.19
3 (0.15 s)	668	288	15.31
4 (0.20 s)	380	120	13.94
5 (0.25 s)	160	64	4.39
6 (0.30 s)	96	21	4.65
7 (0.35 s)	75	44	7.20
8 (0.40 s)	31	7	2.51
9 (0.45 s)	24	3	4.56
10 (0.50 s)	21	1	0.11
11 (0.55 s)	20	3	3.18
12 (0.60 s)	17	2	0.19
13 (0.65 s)	15	0	N/A
14 (0.70 s)	15	3	0.05
15 (0.75 s)	12	1	1.11
16 (0.80 s)	11	2	1.66
17 (0.85 s)	9	1	1.37
18 (0.90 s)	8	3	0.23
19 (0.95 s)	5	3	0.16
20 (1.00 s)	2	2	0.01
APS	3.111 cycle (0.1556 s)	APE	12.43

Another merit of the proposed hybrid probabilistic predictor model is combining the ELM with RVFL advantages, so that the proposed model has better learning diversity. From Fig. 9, it is obvious that the single ELM ensemble model has smaller MAPE, but the speed of this model is lower. In contrast to the single ELM ensemble model, a single RVFL ensemble model has a faster speed, but the MAPE is larger. By combining these two different algorithms, the proposed hybrid probabilistic predictor has both faster speed and less MAPE, meaning higher accuracy.

5.4 Online application testing results

With the proposed hybrid ensemble model, the FIDVR severity of the testing instances is evaluated via the 20 probabilistic predictors. Among these Pareto points of the proposed hybrid model, a compromise solution is chosen to represent the optimal FIDVR results. In this case study, a practical industry requirement of 15.00% is set for APE, which can truly regulate the FIDVR error.

To demonstrate the better performance of the time-adaptive framework, seven different FIDVR testing instances are randomly chosen from the testing instances, and the true TVSI and the predicted TVSI at T_1, T_5, T_{10}, T_{19} are shown in Table 3. It can be clearly observed that the predicted TVSI values at T_1 and T_{19} are the totally farthest and totally nearest from the true TVSI values, demonstrating the decrease in prediction and decision at a later time point.

Based on such a practical requirement, the Pareto point of the proposed hybrid model shown in Table 4 is utilised as the compromise solution since it satisfies the 15.00% APE requirement with the lowest APS. In practical applications, the selection of the compromise Pareto point may not be subject to the above strategy. It is available for decision-makers to use their own strategies to select a compromise Pareto point. Meanwhile, they need to adjust their choices according to the practical FIDVR assessment needs of power systems. Thus, the proposed hybrid model provides the decision-makers more flexibility in manipulating the assessment performance, which can make the proposed model more suitable for real-world FIDVR assessment.

The proposed hybrid method is employed to test its online FIDVR performance by using the testing instances. The testing result is listed in Table 5. From left to right, the columns of Table 5 are the time point, the number of remained samples evaluated at the *i*th time point, the number of evaluated samples at the *i*th time point, and the assessment accuracy, respectively. Besides, the last row shows the APS and APE.

The APE and APS in Table 5 are extremely close to the validated assessment results in Table 4. More specifically, the APS in the testing result is slightly higher, but the APE is significantly lower, which can further demonstrate the trade-off relationship between FIDVR speed and error.

6 Conclusion

This paper proposes an optimised hybrid ensemble probabilistic time-adaptive method for real-time FIDVR assessment. For the proposed method, different randomised ML algorithms (ELM and RVFL), are constructed to design a hybrid ensemble learning model which can provide more diversified ML output. The assessment decision under a time-adaptive prediction framework would be obtained as fast as possible without sacrificing FIDVR assessment accuracy. In order to achieve the above performance, TVSI, as an evaluation of the FIDVR severity, is probabilistically predicted at each point time, and the assessment decision would be made when the prediction result satisfies the credibility condition. Moreover, the FIDVR assessment performance is optimised via coping with a MOP to pursue the optimally balanced the accuracy and speed.

Compared with the single ensemble methods, the proposed method can improve FIDVR assessment results, so that the subsequent emergency control actions can be activated earlier, verifying the feasibility of the proposed optimised hybrid ensemble probabilistic time-adaptive method.

7 Acknowledgments

The work of this paper was supported in part by ARC Research Hub for Integrated Energy Storage Solutions Project ID: IH180100020, Ren Chao's work was supported by Nanyang Technological University, Singapore.

8 References

[1] NERC Transmission Issues Subcommittee and System Protection and Control Subcommittee: 'Fault-induced delayed voltage recovery'. Technical Reference Paper Princeton, NJ, USA, June 2009, version 1.2

[2] Banakar, H., Luo, C., Ooi, B.T.: 'Impacts of wind power minute-to-minute variations on power system operation', *IEEE Trans. Power Syst.*, 2008, **23**, (1), pp. 150–160

[3] Potamianakis, E.G., Vournas, C.D.: 'Short-term voltage instability: effects on synchronous and induction machines', *IEEE Trans. Power Syst.*, 2006, **21**, (2), pp. 791–798

[4] U. S. Department of Energy Workshop: 'On the role of residential AC units in contributing to fault-induced delayed voltage recovery', 22 April 2008

[5] AEMO: 'Black system South Australia 28 Sep 2016'. 3rd Preliminary Report, VIC, Australia, December 2016. Available at https://www.aemo.com.au/-/media/Files/Electricity/NEM/Security_and_Reliability/Reports/Integrated-Third-Report-SA-Black-System-28-September-2016.pdf

[6] Glavic, M., Novosel, D., Heredia, E.*, et al.*: 'See it fast to keep calm: real-time voltage control under stressed conditions', *IEEE Power Energy Mag.*, 2012, **10**, (4), pp. 43–55

[7] Dong, Y., Xie, X., Wang, K.*, et al.*: 'An emergency-demand-response based under speed load shedding framework to improve short-term voltage stability', *IEEE Trans. Power Syst.*, 2017, **32**, (5), pp. 3726–3735

[8] Halpin, S., Harley, K., Jones, R.A.*, et al.*: 'Slope-permissive under-voltage load shed relay for delayed voltage recovery mitigation', *IEEE Trans. Power Syst.*, 2008, **23**, (3), pp. 1211–1216

[9] Bai, H., Ajjarapu, V.: 'A novel online load shedding strategy for mitigating fault-induced delayed voltage recovery', *IEEE Trans. Power Syst.*, 2011, **26**, (1), pp. 294–304

[10] Dasgupta, S., Paramasivam, M., Vaidya, U.*, et al.*: 'Real-time monitoring of short-term voltage stability using PMU data', *IEEE Trans. Power Syst.*, 2013, **28**, (4), pp. 3702–3711

[11] Zhu, L., Lu, C., Sun, Y.: 'Time series shapelet classification based online short-term voltage stability assessment', *IEEE Trans. Power Syst.*, 2016, **31**, (2), pp. 1430–1439

[12] Zhu, L., Lu, C., Dong, Z.Y.*, et al.*: 'Imbalance learning machine based power system short-term voltage stability assessment', *IEEE Trans. Indu. Inf.*, 2017, **13**, (5), pp. 2533–2543

[13] Pinzón, J.D., Colomé, D.G.: 'Real-time multi-state classification of short-term voltage stability based on multivariate time series machine learning', *Int. J. Electr. Power Energy Syst.*, 2019, **108**, pp. 402–414

[14] Zhu, L., Lu, C., Liu, Y.*, et al.*: 'Wordbook-based light-duty time series learning machine for short-term voltage stability assessment', *IET Gener. Transm. Distrib.*, 2017, **11**, (18), pp. 4492–4499

[15] Xu, Y., Zhang, R., Zhao, J.*, et al.*: 'Assessing short-term voltage stability of electric power systems by a hierarchical intelligent system', *IEEE Trans. Neural Netw. Learn. Syst.*, 2016, **27**, (8), pp. 1686–1696

[16] Zhang, R., Xu, Y., Dong, Z.Y.*, et al.*: 'Post-disturbance transient stability assessment of power systems by a self-adaptive intelligent system', *IET Gener. Transm. Distrib.*, 2015, **9**, (3), pp. 296–305

[17] Yu, J.J.Q., Hill, D.J., Lam, A.Y.S.*, et al.*: 'Intelligent time-adaptive transient stability assessment system', *IEEE Trans. Power Syst.*, 2018, **33**, (1), pp. 1049–1058

[18] Zhang, Y., Xu, Y., Dong, Z.Y.*, et al.*: 'Real-time assessment of fault-induced delayed voltage recovery: a probabilistic self-adaptive data-driven method', *IEEE Trans. Smart Grid*, 2019, **10**, (3), pp. 2485–2494

[19] Khamis, A., Xu, Y., Dong, Z.Y.*, et al.*: 'Fast detection of microgrid islanding events using an adaptive ensemble classifier', *IEEE Trans. Smart Grid*, 2018, **9**, (3), pp. 1889–1899

[20] Shoup, D.J., Paserba, J.J., Taylor, C.W.: 'A survey of current practices for transient voltage dip/sag criteria related to power system stability'. Proc. IEEE PES Power Systems Conf. Exposition, New York, NY, 2004, pp. 1140–1147

[21] Ren, C., Xu, Y., Zhang, Y.: 'Post-disturbance transient stability assessment of power systems towards optimal accuracy-speed trade-off', *Prot. Control Mod. Power Syst.*, 2018, **3**, (1), p. 19

[22] Xu, Y., Dong, Z.Y., Zhao, J.H.*, et al.*: 'A reliable intelligent system for real-time dynamic security assessment of power systems', *IEEE Trans. Power Syst.*, 2012, **27**, (3), pp. 1253–1263

[23] Schmidt, W.F., Kraaijveld, M.A., Duin, R.P.W.: 'Feedforward neural networks with random weights'. Proc. 11th IAPR Int. Conf. on Pattern Recognition. Vol. II. Conf. B: Pattern Recognition Methodology and Systems, The Hague, Netherlands, 1992, pp. 1–4

[24] Huang, G.-B., Zhu, Q.-Y., Siew, C.-K.: 'Extreme learning machine: theory and applications', *Neurocomputing*, 2006, **70**, (1), pp. 489–501

[25] Zhang, L., Suganthan, P.N.: 'A comprehensive evaluation of random vector functional link networks', *Inf. Sci.*, 2016, **367–368**, pp. 1094–1105

[26] Ren, C., Xu, Y., Zhang, Y.*, et al.*: 'A multiple randomized learning based ensemble model for power system dynamic security assessment'. 2018 IEEE Power & Energy Society General Meeting (PESGM), Portland, OR, 2018, pp. 1–5

[27] Ren, C., Xu, Y., Zhang, Y.*, et al.*: 'A hybrid randomized learning system for temporal-adaptive voltage stability assessment of power systems', *IEEE Trans. Ind. Inf.*, 2020, **16**, (6), pp. 3672–3684

[28] Zhou, Z.-H., Wu, J., Tang, W.: 'Ensembling neural networks: many could be better than all', *Artif. Intell.*, 2002, **137**, (1–2), pp. 239–263

[29] Deb, K., Pratap, A., Agarwal, S.*, et al.*: 'A fast and elitist multi-objective genetic algorithm: NSGA-II', *IEEE Trans. Evol. Comput.*, 2002, **6**, (2), pp. 182–197

[30] Siemens Power Technologies International, PSS®E 33.0 Program Application Guide: Volume-II, March 2013

[31] Zhang, R., Xu, Y., Dong, Z.Y.: 'Measurement-based dynamic load modelling using time-domain simulation and parallel-evolutionary search', *IET Gener. Transm. Distrib.*, 2016, **10**, (15), pp. 3893–3900